Received: 12 July 2021 | Revised: 30 September 2021 | Accepted: 2 October 2021

DOI: 10.1002/app.51816

ARTICLE

Applied Polymer SCIENCE WILEY

Extrusion foaming behavior of polybutene-1. Toward single-material multifunctional sandwich structures

Lucía Doyle

Infrastructural Engineering, HafenCity University, Hamburg, Germany

Correspondence
Lucía Doyle, Infrastructural Engineering, HafenCity University, Henning-Voscherau-Platz 1, 20457 Hamburg, Germany.
Email: lucia.doyle@hcu-hamburg.de

Funding information
HafenCity University

Abstract

Polymeric foams are a key element of many multifunctional sandwich structures. The most commonly used polymeric foam, polyurethane, presents environmental drawbacks, related to poor recyclability and the use of toxic diisocyanates for their manufacturing. The separation of layers in sandwich structures is a further unresolved hurdle toward the recyclability of these elements. There is a need for broadening the spectrum of polymeric foams. In this context, the foamability of polybutene-1 (PB-1) is studied through extrusion foaming experiments. From the application side, foaming PB-1 would allow the manufacturing of district heating pre-insulated pipes out of one single material, bringing circular product design to the energy sector. From the scientific side, there is a knowledge gap in the foaming of polymers in the rubbery state at room temperature, such as PB-1, due to difficulties in the cell stabilization step. This supports the need for research in the foaming of this polymer. In this study, four commercial grades of PB-1 were evaluated, covering different chain structures, molecular weights, and crystallinity degrees. Very different foaming behaviors were found. Dimensionally stable foams were achieved with the two homopolymers tested, demonstrating the foamability of this polymer.

KEYWORDS

extrusion, foams, polyolefins, circular economy, circular product design

1 | INTRODUCTION

Polymeric foams have experienced an increased use in recent years as a key element in multifunctional sandwich structures, which combine a structural load-bearing function with nonstructural functions like insulation. This has expanded their use in applications including aerospace,[1–4] marine,[5–7] civil,[6–9] and energy infrastructure as wind blades[10,11] and district heating piping networks.[12]

Most commonly used polymeric foams such as polyurethane (PU) are thermoset, hindering their recyclability, as well as require hazardous raw materials for their manufacturing, such as the recently restricted diisocyanates in PU.[13,14] Analogously to how the phasing out of chlorofluorocarbons (CFCs) enforced by the Montreal Protocol[15] triggered research and development on alternative blowing agents during the 90s and 2000s,[16–20] pressing requirements on material's recyclability and environmental impact brought by the circular economy has placed research and use of thermoplastic,[21–28] biodegradable,[29–31] and biobased[32–34] foams on the current research agenda. However, the recyclability of sandwich structures is hindered by the separation of the different layers of materials, which is

still an unresolved problem. A true transition to the circular economy involves a holistic product design, evaluating the recyclability of the complete composite structure and not only of its individual layers. Best practice in green engineering includes minimization of the number of materials in an element.[35] This could be achieved by increasing the knowledge on foaming of a broader range of polymers, tailoring the properties of multifunctional structures not by material layers but by material processing.

Polybutene-1 (PB-1) is a polyolefin produced by the polymerization of 1-butene using supported Ziegler–Natta catalysts.[36] It is a high-molecular weight, linear, isotactic, and semicrystalline polymer. Properties include low coefficient of thermal expansion,[12] high-heat deflection temperature, stress cracking resistance (ESCR), and outstanding creep resistance.[37] It is a recyclable thermoplastic and nontoxic,[38] pre-requisites for circular product development.

PB-1 is one of the common materials used as service pipes for district heating networks,[12,39] application which motivates this research. Current district heating pre-insulated pipes are sandwich components comprising a service pipe and foam layer, as for state-of-the-art of PU,[39] and a protective casing. The foam layer acts both as insulation and as bond between the medium pipe and the casing, supporting multiaxial stresses. Currently used PU in bonded pre-insulated pipes is required to have a thermal conductivity lower than 0.029 W/(m × K),[40] and for insulated plastic pipes, an axial shear strength >0.09 MPa.[41] Foaming PB-1 would allow the manufacturing of a pre-insulated pipe out of only one material.

From the scientific perspective, with a glass transition temperature (T_g) of −25°C,[37] PB-1 is a polymer in the rubbery state at room temperature, a polymer class for which limited studies on foaming exist, and an identified challenge in foaming.[42] This is due to the difficulty in the cell stabilization step, as a result post-foaming shrinkage due to the escape of the blowing agent from the matrix, facilitated by being above its T_g, and cell coalescence driven by viscoelasticity. There is a need for increasing the knowledge on foam processing for this polymer class.

After an extensive literature search for PB-1 foaming, only one reference was found, were one grade of PB-1 was included in a screening of different semicrystalline polymers targeted to assess the effects of crystallinity on the morphology of foams prepared by temperature-induced batch foaming.[43] This highlights the need for research on the foaming behavior of this polymer.

In this study, the extrusion foaming behavior of PB-1 is studied using a chemical blowing agent (CBA). Different commercial grades were evaluated, including two homopolymers, one copolymer, and one thermoplastic elastomer. The obtained samples have been characterized for density, expansion ratio, and microstructure. Foamability is assessed in terms of achieved volume expansion ratio, microstructure, and processing window size, using available extrusion equipment. Optimization of the foaming process is out of the scope of this study. A part of this study was presented in the First International Conference on "Green" Polymer Materials 2020 [44] and included here for completeness.

Very different foaming behavior has been found between the tested grades. The two homopolymers presented the better foaming behavior. Foams with cell population density of 10^4 cells/cm^3 and expansion ratio of up to 1.8 were obtained, demonstrating the foamability of the polymer. The processing window was found to be narrow, as expected for a linear semicrystalline polymer. Foam shrinkage, one of the identified main risks given the rubbery nature of PB-1, was found in the thermoplastic elastomer grade only. The tested homopolymers presented good dimensional stability. The main challenge to overcome is the low-melt strength, as encountered in recent developments of polypropylene (PP),[22,45] polyethylene terephthalate (PET),[28,30,46] or polylactic acid (PLA) foams,[34] which limits volume expansion. Higher expansion ratios could be obtained through processing optimization and resin rheology improvements, through, that is, increasing the molecular weight of the polymer.

2 | EXPERIMENTAL

2.1 | Materials

Four commercial grades of PB-1 from LyondellBasell were investigated, presenting different chain structures, molecular weights, degree of crystallinity (X_c), melting temperature (T_m), and melt flow ratio (MFR). Table 1 presents an overview with the data provided by the manufacturer. Resins were used as received.

A chemical blowing agent (CBA) was used, Hydrocerol CT 550, kindly provided by Clariant. The amount of dosed CBA was varied between 2% and 10%. The main gas released by this CBA is CO_2, and the effective components amount to 70% according to the technical data sheet.

2.2 | Sorption/desorption kinetics

Sorption and desorption kinetics of CO_2 in PB1-a, PB1-b, and PB1-c at room temperature were studied using the gravimetric method proposed by Berens & Huvard.[47] CO_2 of >99.8% purity was used. The polymer was molten and compression molded into discs of 40 mm diameter

TABLE 1 Overview of the evaluated PB-1 resins

Resin	Type	Approx. molecular weight (g/mol)	X_c (%)	T_m	MFR (g/10 min @190°C/2.16 kg)
PB1-a	Homopolymer	530,000	~55	128°C	0.4
PB1-b	Homopolymer	460,000	~55	131°C	0.6
PB1-c	Thermoplastic elastomer	550,000	~25	114°C	0.5
PB1-d	Random copolymer	315,000	~35	97°C	2.5

Abbreviation: PB1, polybutene-1.

and 2 mm thickness. PB-1 experiences crystal–crystal transformation at room temperature. When cooling from the melt, it crystallizes into metastable Form II, characterized by a tetragonal unit cell. They then gradually transform into Form I stable crystals.[48–50] This process is completed in around 10 days depending on the storage conditions.[51] Therefore 10 days were allowed between the sample molding and sorption/desorption tests, as to test in the same form as the as-received pellets in the extrusion experiments. The discs where saturated at room temperature and 50 bars in an autoclave (Eurotechnica GmbH, Bargteheide, Germany). This pressure was selected as to be close to the extruder die pressure. Once the defined saturation time (t_s) was reached, a rapid decompression of <30s was undertaken. The samples were placed in an analytical balance with sensitivity of at least 1 mg and its weight decrease logged in 5 s intervals.

From the initial disk weight before sorption, W_0, and the weight recorded during desorption (W_t), the rate of desorbed CO_2, $M_{t,d}$, can be derived as:

$$M_{t,d} = \frac{(W_t - W_0)}{W_0}. \quad (1)$$

For Fickian diffusion from a plane sheet,[52] the plot of $M_{t,d}$ versus $\sqrt{t_d}$ is initially linear, and extrapolation to desorption time $t_d = 0$ provides $M_{t,s}$, the sorbed CO_2 at the end of the sorption period t_s. By running consecutive tests for longer t_s, the equilibrium uptake M_∞ is found once a constant value of $M_{t,s}$ is obtained. Experiments were conducted in triplicate.

2.3 | Extrusion foaming process

A twin screw ZSE 27 MAXX extruder (Leistritz Extrusionstechnik GmbH, Nürnberg, Germany) was used, with D = 28.3 mm, L/D = 48, and 12 modular barrels with 2.1 kW heating power each and water cooling. A strand die with three strands of 4 mm diameter each was used. The feeding temperature was set as low as possible as to create a melt seal and avoid premature degassing of the CBA, which was set between 130 and 145°C depending on the resin used. The temperature was progressively increased up to 175°C until after the CBA dosing point, as to allow its complete decomposition. From then on, it was progressively lowered. Die exit temperatures were varied between 80 and 140°C. Die pressure was monitored. Preliminary trials were conducted to determine adequate mass flow rate and screw speed for foaming with the available extruder and screw configuration. 100 rpm and 4 kg/h were found appropriate to achieve the necessary die pressure for foaming to occur.

2.4 | Foam characterization

The foam samples were randomly collected at each processing condition and characterized for dimensional stability, volume expansion, density, cell size, and cell population density.

The dimensions stability of the extrudates was evaluated by photographing the strands using a Nikon D700 camera from immediately after collection (time between collection and initial photo max 20s) up to over 2 h after extrusion, in 20 s intervals. The diameter of each strand through the sequence was then measured from the images at least three different points and the average reported.

The density of the extrudates was determined in triplicate with a 100 ml glass pycnometer, distilled water and a Sartorius AC 211 S (Göttingen, Germany) balance.

The volume expansion ratio (V_{exp}) was calculated as

$$V_{exp} = \frac{\rho\,\text{polymer}}{\rho\,\text{foam}}. \quad (2)$$

The morphology of the foams was examined in an optical microscope (Leica DMLP, Wetzlar, Germany). Cell size was measured from the obtained micrographs using the open-source image-processing package Fiji.[53] Measurements from around 100 cells and typically three micrographs per resin and process conditions are reported.

Cell population density, defined as the number of cells per unit volume of the original unfoamed polymer, was calculated as:[29,54]

$$N_0 = \left(\frac{n}{A}\right)^{3/2} \cdot V_{exp}, \quad (3)$$

where (N_0) is the cell population density (cell/cm^3), n is the number of cells in the micrograph and A the area of the micrograph (cm^2) and V_{exp} the volume expansion ratio.

3 | RESULTS

3.1 | Sorption/desorption kinetics

Figure 1a presents the desorption curves for grades PB1-a, PB1-b, and PB1-c for samples sorbed up to equilibrium, and Figure 1b the CO_2 uptake versus sorption time. It can be readily observed that PB1-a and PB1-b present very similar CO_2 sorption/desorption kinetics, with a linear desorption profile. PB1-c presents a significantly different behavior, with an exponential decay desorption profile. Practically the totality of the sorbed CO_2 is desorbed in approximately 6 min, for all the sorption times trialed. This has a great impact on the foam dimensional stability, as will be described in the following sections. A slight combing of the PB1-c disks upon extraction from the autoclave could be also observed, as well as a change in color from translucid to white (see Figure 2).

Changes in light transmission intensity through polymer sheets have been related to lamellar thickening and recrystallization induced by CO_2.[55]

From the $M_{t,s}$ data (see Table 2) it can be also concluded that the solubility of CO_2 is higher in PB1-c. Due to the rapid desorption, the extrapolation to $t_d = 0$ is

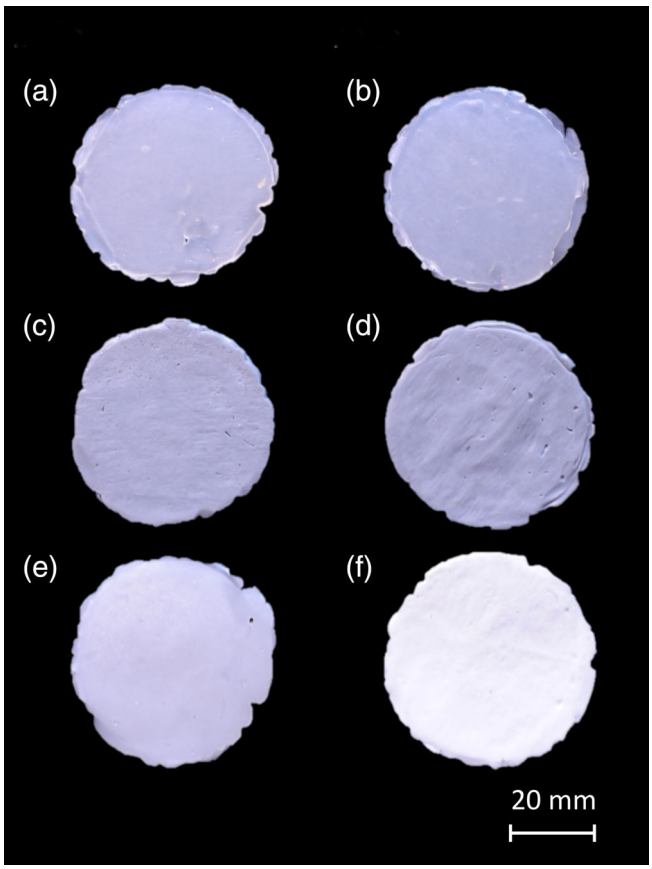

FIGURE 2 Samples of PB1-a before (a) and after (b) sorption/desorption, PB1-b before (c) and after (d), and PB1-c before (e) and after (f) sorption/desorption test. PB1, polybutene-1 [Color figure can be viewed at wileyonlinelibrary.com]

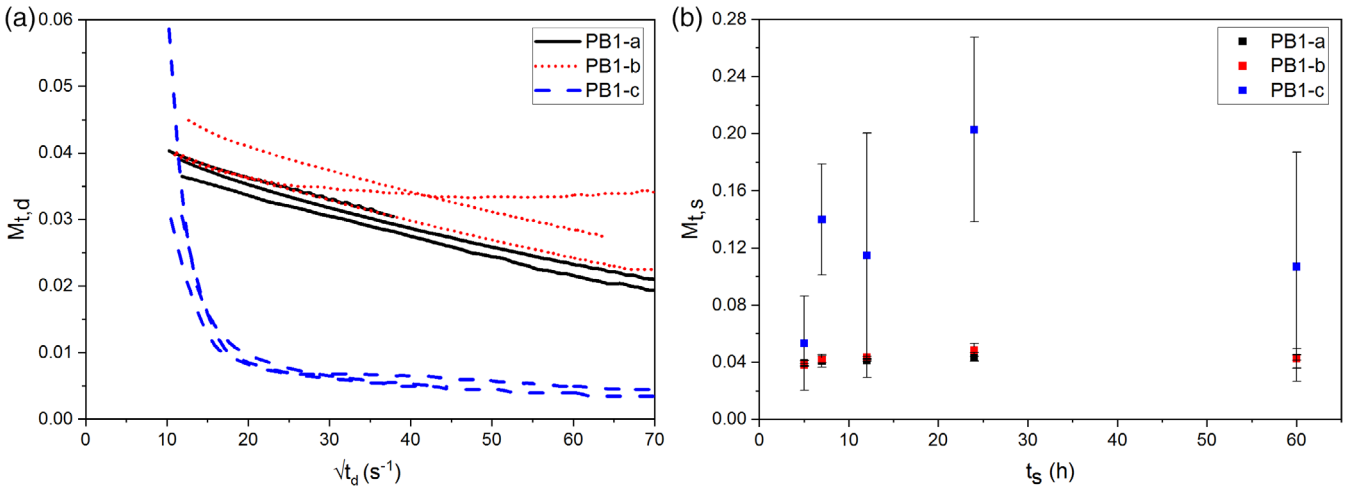

FIGURE 1 (a) Desorption curves after 24 h sorption time (sorption equilibrium reached) and (b) mass uptake versus sorption time [Color figure can be viewed at wileyonlinelibrary.com]

more imprecise than for resins PB1-a and PB1-b, and therefore the higher variability in the results. For a higher precision, an in situ measurement would be required, such as a magnetic suspension balance. The obtained results allow to explain the dimensional stability behavior of the post-extruded foam strands.

3.2 | Foaming behavior

PB1-a and PB1-b produced dimensionally stable foam extrudates. Processing temperature window was narrow in both cases. For resin PB1-a, above 115°C die temperature, rupture of the extrudate's skin and limited expansion could be visually observed, implying low-melt strength to withstand bubble growth above that temperature. The lower operating temperature was found to be 110°C, temperature below which the extrudates would solidify at the die exit. A relatively high-CBA dose was needed to visually obtain a significant volume expansion.

TABLE 2 Rate of CO_2 desorption after different saturation times

	$M_{t,s}$		
t_s (h)	PB1-a	PB1-b	PB1-c
5	0.039 ± 0.002[a]	0.038 ± 0.001[a]	0.053 ± 0.033[a]
7	0.041 ± 0.004[a]	0.042 ± 0.002[a]	0.140 ± 0.039[a]
12	0.041 ± 0.001[a]	0.043 ± 0.001[a]	0.115 ± 0.086[a]
24	0.044 ± 0.003[a]	0.049 ± 0.005[a]	0.203 ± 0.065[a]
60	0.043 ± 0.002[a]	0.043 ± 0.007[a]	0.107 ± 0.080[a]

Abbreviation: PB1, polybutene-1.
[a]SD.

Resin PB1-b presented a slightly wider processing temperature window, with an equivalent behavior than PB1-a on the low end, but the upper temperature could be increased to 120°C, temperature above which gas escape from the extrudate's skin could be visually observed. A higher die swell could be observed with this resin, and its implications covered in Section 4.

The processing window for resin PB1-c was very narrow, limited by the high viscosity on the low end and high-gas diffusivity on the high end. With die temperature from 110°C onwards, gas escaping from the extrudate skin could be visually observed, leading to very low-expansion ratio, and below 100°C high-viscosity prevented processing. Foam extrudates with visually acceptable expansion ratio were obtained with a die

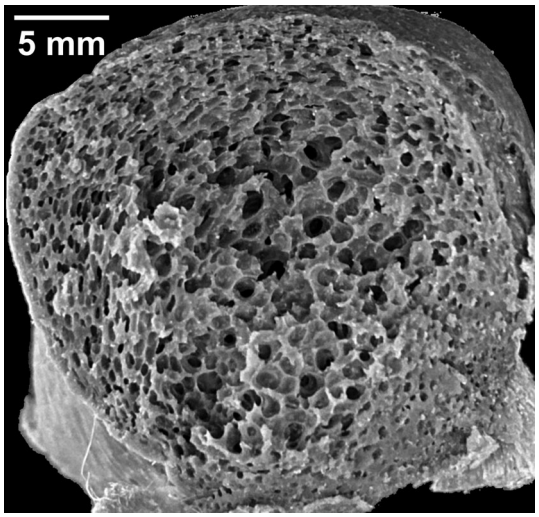

FIGURE 4 Photograph of extrudate section, corresponding to PB1-b, die T = 110°C. PB1, polybutene-1

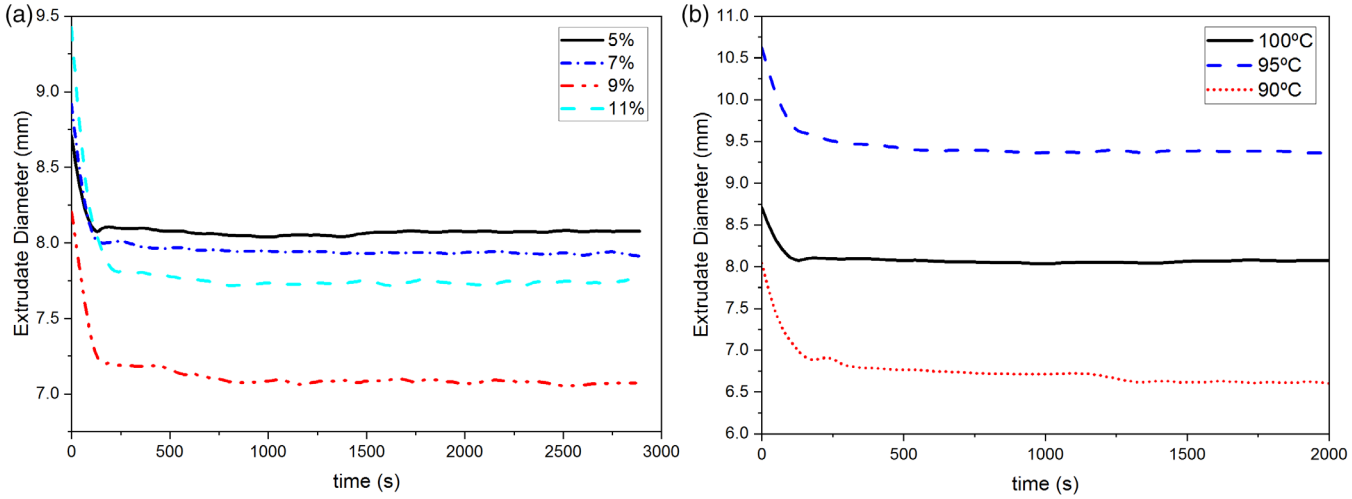

FIGURE 3 Extrudate diameter of PB1-c versus time, for different CBA concentrations at die T = 100°C (a) and 5% CBA and different die T (b). CBA, chemical blowing agent; PB1, polybutene-1 [Color figure can be viewed at wileyonlinelibrary.com]

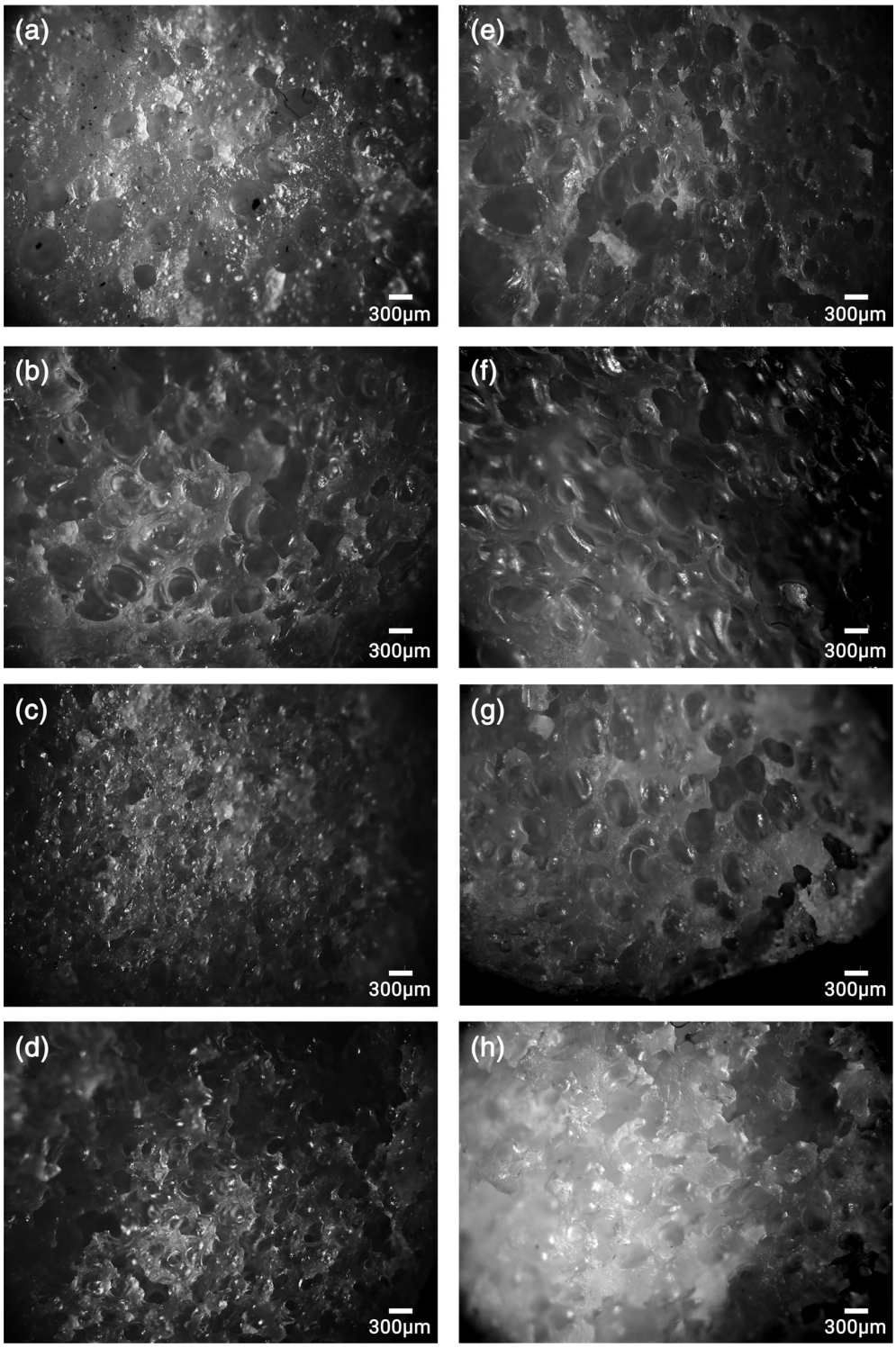

FIGURE 5 Micrographs obtained from PB1-a: (a) die T = 110°C and 4.2% CBA, (b) 7.15%, (c) 8.6%, and (d) 10% CBA; (e) die T° = 115°C and 4.2%, (f) 7.15%, (g) 8.6%, (h) 10%. CBA, chemical blowing agent; PB1, polybutene-1

temperature of 100°C. However, severe post-foaming shrinkage was observed. Figure 3 shows the evolution of the diameter width with time after extrusion, for different CBA concentrations at 100°C die temperature (a) and for 5% CBA and different die temperature (b).

As can be seen, most of the shrinkage occurred in the first 2.5 min after foaming, irrespective of the CBA concentration used. This can be directly related to the CO_2 diffusivity of PB1-c, see Figure 2a). Given the poor dimensional stability, this grade was excluded from further characterization.

The foam extrusion of PB1-d was screened with die temperature between 80 and 110°C. Foaming was not achieved, and obtained extrudates presented low viscosity and dimensional stability. Therefore, this grade was excluded from further analysis.

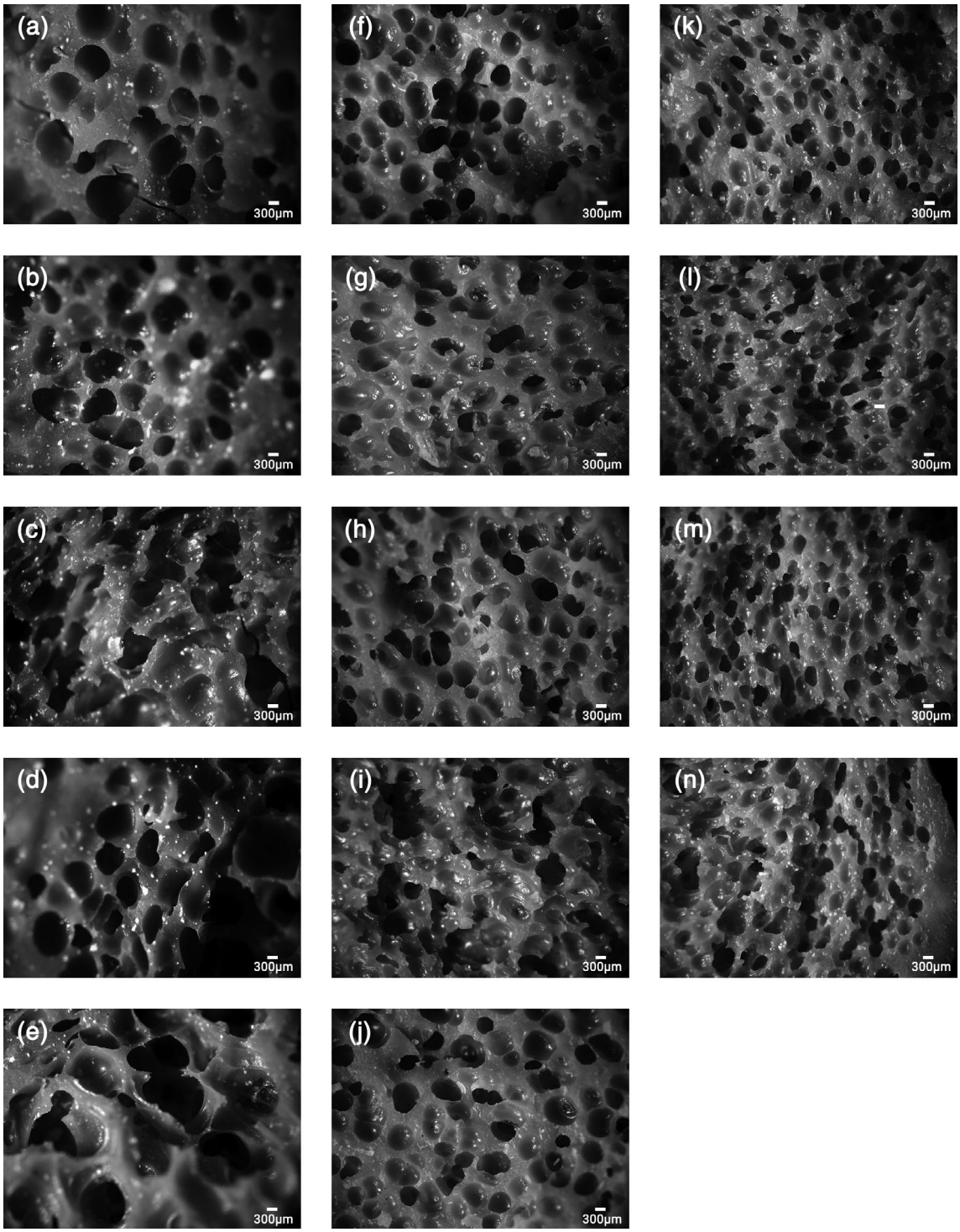

FIGURE 6 Micrographs obtained from PB1-b: (a) die T = 110°C and 2%, (b) 3%, (c) 4.2%, (d) 5.5%, and (e) 7% CBA; (f) die T° = 115°C and 2%, (g) 3%, (h) 4.2%, (i) 5.5%, and (j) 7% CBA; and (k) die T° 120°C 2% CBA, (l) 4.2%, (m) 5.5%, and (n) 7% CBA. CBA, chemical blowing agent; PB1, polybutene-1

3.3 | Foam characterization

The obtained foam extrudates present a skin and a gradient in cell size. This is due to the low-die temperatures used, which solidifies the skin and produces a Joule-Thompson like cooling at the outer surface.[56] A photograph of an example extrudate section is presented in Figure 4.

Representative micrographs for each process condition for grades PB1-a can be found in Figure 5 and for PB-1b in Figure 6.

The determined volume expansion ratio, cell diameter and cell population density their relation with the process conditions are presented in Figure 7a–c for PB1-a and Figure 7d–f for PB1-b. It should be noted that given the shape irregularity, the reported diameter is the equivalent diameter, defined as the diameter of a circle with the same area as the measured cell area.

The obtained foam densities can be found in Table 3. It should be noted that a CBA is used, for which the effective foaming components amount to 70% weight (wt). Therefore, some mass is added due to the decomposition products, contributing to the density of the obtained foam. The calculated expansion ratio is therefore slightly underestimated.

As can be observed in Figures 5, 6, and 7b,e, foams present large pores with significant cell size variability.

For PB1-a, the two die temperatures set did not produce any difference in the obtained cell size for CBA concentrations of 4.2 and 7.1% wt. Cell size decreased for 8.5% wt as cell population density increased. This inverse relationship is consistent with the reports of previous authors.[57,58] This effect is particularly notorious for the 110°C die temperature trial, where the average cell size was reduced by more than 50%. After this point N_0 decreased again and cell size increased. This can be explained as the increase of CBA provides more available gas for cell nucleation, until a maximum is reached. With further gas increase and cell growth, cells collide against each other, reducing the number of cells and increasing their size,[59] as can be observed in the trends of Figure 7b, c. As for the expansion ratio, as can be seen in Figure 7a); with the die temperature of 110°C, it increased until a maximum and then decreased. This indicated that at this temperature the expansion behavior is governed by the polymer melt's stiffness. The expansion increase with increasing CBA concentration can be related to the plasticization effect of the gas.[57] After reaching a maximum, the gas starts diffusing out of the polymer's hot skin, leading to a reduced expansion. For the 115°C die temperature series, the maximum expansion was achieved with the lowest concentration of CBA tested, remaining at constant levels until the last CBA concentration tested, of 10%, where the expansion decreased. It can be derived that above that dosage the increased level of gas just increased the diffusion out of the hot skin of the extrudates, thus the volume expansion remained at constant levels. The final expansion reduction together with reduction of N_0 is an indication of cell coalescence.

For PB1-b, the same inverse relationship between cell size and N_0 can be observed. With this resin, foaming could be visually observed at lower CBA doses than for PB1-a. In Table 1 it can be seen that the MFR is lower for PB1-a than for PB1-b. MFR is an indirect measurement of viscosity, being the two parameters inversely proportional. Therefore, this difference could be related to the higher viscosity of PB1-a, requiring higher CBA concentration to achieve expansion. It can be seen in Figure 7f) that the cell population density is in general higher with higher die temperature. This could be related to reduced stiffness with higher temperatures, which favorizes cell nucleation and growth.

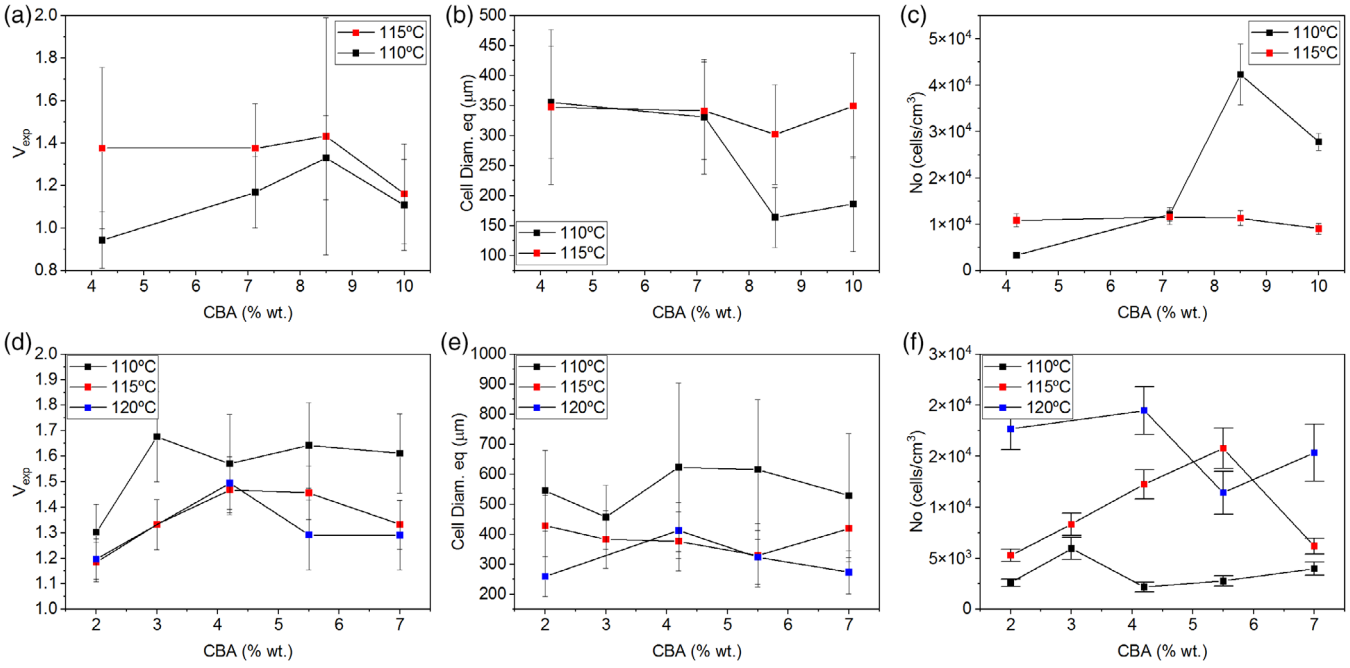

FIGURE 7 Relationship of the processing conditions with volume expansion ratio (a), cell equivalent diameter (b) and cell population density (c) for PB1-a, and same in (d), (e), and (f) for PB1-b. PB1, polybutene-1 [Color figure can be viewed at wileyonlinelibrary.com]

TABLE 3 Density of the obtained foams

	(CBA) % wt	Die T° (°C)	Density (g/cm^3)
PB1-a	4.2	110	0.74 ± 0.03
	7.1	110	0.50 ± 0.02
	8.5	110	0.60 ± 0.03
	10.0	110	0.52 ± 0.03
	11.2	110	0.63 ± 0.09
	4.3	115	0.51 ± 0.12
	7.2	115	0.51 ± 0.04
	8.6	115	0.49 ± 0.18
	10.1	115	0.60 ± 0.09
PB1-b	2	110	0.61 ± 0.02
	3	110	0.47 ± 0.04
	4.2	110	0.50 ± 0.05
	5.5	110	0.48 ± 0.03
	7	110	0.49 ± 0.03
	2	115	0.67 ± 0.01
	3	115	0.59 ± 0.02
	4.2	115	0.54 ± 0.01
	5.5	115	0.54 ± 5.5
	7	115	0.59 ± 0.08
	2	120	0.60 ± 0.01
	4.2	120	0.48 ± 0.01
	5.5	120	0.56 ± 0.05
	7	120	0.56 ± 0.05

Abbreviations: CBA, chemical blowing agent; PB1, polybutene-1.

TABLE 4 Die swell

	d (cm)	B_{exp}
PB1-a	0.99 ± 0.06	2.48 ± 0.15
PB1-b	1.09 ± 0.06	2.73 ± 0.15

Abbreviation: PB1, polybutene-1.

As for volume expansion ratio, the highest level for this grade is achieved with the lowest die temperature. Expansion ratio is related to both cell size and cell population density. In this case, it can be seen that the volume expansion is driven by a low number of very large cells.

4 | DISCUSSION

4.1 | Effect of resin type in foaming behavior

A very different foaming behavior was found between the four different grades tested. This highlights how a broad screening of different grades is required in order to assess the foamability of a particular polymer. Of the four grades tested, the two homopolymers PB1-a and PB1-b present better foaming behavior. The thermoplastic elastomer PB1-c failed in terms of dimensional stability, severely suffering from post-foaming shrinkage. This was an identified risk,[42] related to the rubbery state of PB-1, which was however found in this grade only. From the study of the CO_2 desorption kinetics, it is clear that this shrinkage is related to the high diffusivity, leading to a quick gas escape before the matrix can solidify. Further information on the chain configuration would be required to explain the significantly different desorption kinetics between PB1-c and the two homopolymers. The lower crystalline content (see Table 1) can be pointed out as a contributor toward higher solubility and diffusivity.

The lack of foaming ability of PB1-d can be related to its low viscosity, which hinders the matrix from withstanding the stretching forces required for bubble growth.[60]

A similar volume expansion ratio was achieved with PB1-a and PB1-b. Both grades allowed the foaming of dimensionally stable foam extrudates, which was one of the main research questions of this study. The CO_2 diffusivity has been found equivalent for both resins. PB1-b presents a slightly broader processing temperature window than PB1-a.

For PB1-a, cell size is larger for higher die temperatures. This is consistent with the report of previous authors.[61] Interestingly, for PB1-b, the opposite trend is found, with significantly larger cell sizes obtained with the lower die temperatures. It has been noticed that the die swell of PB1-b is higher than for PB1-a, and higher for lower temperatures, where the die swell B_{exp} is defined as:[62]

$$B_{exp} = \frac{d}{d_0}, \tag{4}$$

where d is the measured diameter of the extruded strand and d_0 the diameter of the die.

While for the measurement of the true die swell d should be measured in a complete relaxed strand, requiring some annealing,[62,63] the measurement of the extruded strand diameters provides qualitative data on the die swell, which can be correlated to the degree of elasticity of different samples.[63,64] Therefore, we can see that the PB1-b qualitatively presents higher elasticity than PB1-a, and that lower temperatures allow for a higher melt elasticity, which in turn supports the bubble growth. Table 4 presents the comparison of B_{exp} for PB1-a and PB1-b, obtained with a die temperature of 110°C.

The found correlation between die swell and foaming ability is consistent with the observations of previous authors.[28] It can be seen how multiple variables affect the foaming process, leading to the complexity of its optimization.

4.2 | Foamability of PB-1 versus other polymers

The foaming processing window for PB-1 has been found narrow. This was expected, as PB-1 presents characteristics which have been previously identified as challenging for foaming, such as (a) linear molecular structure, which typically involves the lack of required extensional viscosity to withstand the stretching forces during bubble growth;[60] (b) semicrystallinity, which limits the processing window due to crystallization-induced stiffness on the lower temperatures and insufficient melt strength on the higher temperatures[42] as well as hinders the blowing agent's solubility and diffusivity;[29,43,65] and (c) rubbery state at room temperature, which facilitates the escape of the gas, impacting on the dimensional stability of the foam.[42] It should be noted that some of these features can also be used to the advantage of foaming. For example, while crystallization has significant effects both on cell nucleation mechanisms and cell growth,[29,43] it has been found an effective way to improve the foaming ability of polymers with low-melt strength, as the rigid crystalline structure will help restrict the foam's cell coalescence.[65] An optimal crystallization degree during processing is needed to ensure the foam has a high expansion ratio and a large cell density, and so knowledge on its kinetics. The closest polymer that PB-1 can relate to is PP, as member of the polyolefin family, semicrystalline, and with a T_g below room temperature. Early research on foaming of PP has found the same hurdles described above[22,45] related to the low-melt strength of PP. There is a need to find a processing optimum between allowing for bubble growth and preventing gas loss through the extrudate's hot skin. A successful strategy reported is to keep the die temperature as low as possible as to reduce gas loss during expansion,[24] in common to the findings of our study, where a lower temperature than the recommended processing temperature was used.

It should be noted that the objective of this study is to assess foamability and identify favorable grades for foaming using available extrusion equipment. Hence, optimization of the process conditions is not in the scope of this work. There is room for improving the obtained foam through modifications of both the resin and the extrusion equipment and process.

Early work estimated that the operable temperature range for producing an acceptable PP foam spanned a mere 4°C,[66] range which has been confirmed by later authors.[67] This is narrower than the 10°C found in our study for PB-1. Despite this, successful foaming of PP is reported though the use of branched[24,57] or linear/branched PP blends,[68] reduction of the melt temperature and use of high-molecular weight blowing agents for minimizing gas loss during expansion, adaptation of the processing conditions at the die to match crystallization kinetics[24] and the use of nanoparticles.[69,70] Commercial breakthrough has come with the optimization of processing tools, with the use of strand foam extrusion technology.[71] This method involves the use of a breaker plate, a multi-orifice die producing several individual foam strands, which are then pressed together to yield low-density foam sheets.[72] This enables expanding and stabilizing low-melt strength polymers, and is currently the state-of-the-art technology for commercial PET foam,[72] for which low-melt strength was for long a hurdle toward successful foaming.[28,46,73] There are therefore multiple strategies and pathways open for further optimization and successful development of a PB-1 foam.

5 | CONCLUSIONS

The foam extrusion behavior of four commercial grades of PB-1 was evaluated, including a thermoplastic elastomer, two homopolymers and a random copolymer. Very different behaviors were encountered, highlighting the importance of careful screening with different grades. The two homopolymers were successfully foamed, presenting good dimensional stability and achieving cell population densities of up to 10^4 cells/cm^3 and an expansion ratio of up to 1.8. Foamability was hence confirmed and most promising commercial resins identified. An identified challenge is low-melt strength. Possible optimization strategies to increase the expansion ratio include resin rheology improvements, tailoring processing conditions to the crystallization kinetics and optimizing the extrusion equipment, which will be part of future research.

ACKNOWLEDGMENTS

Prof. Ingo Weidlich is kindly thanked for the discussions and advice during the execution of the research and preparation of the manuscript. Xihua Hu and Prof. Irina Smirnova, from the Technical University of Hamburg, are gratefully thanked for making the extruder available. The Hamburg Energy Research Network (EFH) is kindly acknowledged for facilitating the cooperation. The work reported is self-funded by the HafenCity University. Open Access funding enabled and organized by Projekt DEAL.

ORCID

Lucia Doyle https://orcid.org/0000-0001-8697-8621

REFERENCES

[1] L. R. Lankston, J. A. Wrede, Encapsulated foam for aerospace support applications: Dayton, Ohio, 1964.

[2] E. S. Weiser, F. F. Baillif, B. W. Grimsley, J. M. Marchello, High Temperature Structural Foam, The NASA Headquarters are located in Washington DC, USA **1997**. https://ntrs.nasa.gov/citations/20040110267

[3] E. S. Weiser, T. F. Johnson, T. L. St Clair, Y. Echigo, H. Kaneshiro, B. W. Grimsley, *High Perform. Polym.* **2000**, *12*, 1.

[4] H. F. Seibert, *Reinf. Plast.* **2006**, *50*, 44.

[5] X. Li, Y. Weitsman, *Compos. Part B: Eng.* **2004**, *35*, 451.

[6] L. Hollaway, P. R. Head, *Advanced Polymer Composites and Polymers in the Civil Infrastructure*, Elsevier Science, Amsterdam, London **2001**.

[7] H. Tuwair, J. Volz, M. ElGawady, M. Mohamed, K. Chandrashekhara, V. Birman, *Structures* **2016**, *5*, 141.

[8] A. Manalo, T. Aravinthan, A. Fam, B. Benmokrane, *J. Compos. Constr.* **2017**, *21*, 4016068.

[9] M. Garrido, J. R. Correia, T. Keller, *Constr. Build. Mater.* **2015**, *76*, 150.

[10] O. T. Thomsen, *J. Sandwich Struct. Mater.* **2009**, *11*, 7.

[11] A. Fathi, F. Wolff-Fabris, V. Altstädt, R. Gätzi, *J. Sandwich Struct. Mater.* **2013**, *15*, 487.

[12] R. Wiltshire Ed., *Advanced District Heating and Cooling (DHC) Systems*, Woodhead Publishing Series in Energy, Sawston, United Kingdom **2016**.

[13] European Comission (EU), Commission Regulation (EU) 2020/1149 of 3 August 2020 Amending Annex XVII to Regulation (EC) No 1907/2006 of the European Parliament and of the Council Concerning the Registration, Evaluation, Authorisation and Restriction of Chemicals (REACH) as Regards Diisocyanates **2020**.

[14] J. A. Zapp, *AMA Arch. Ind. Health* **1957**, *15*, 324.

[15] Montreal Protocol on Substances that Deplete the Ozone Layer: Chapter XXVII 2.a, 1987.

[16] W. M. Lamberts, *J. Cell. Plast.* **1992**, *28*, 584.

[17] P. P. Barthelemy, A. Leroy, J. A. Franklin, L. Zipfel, W. Krücke, *J. Cell. Plast.* **1995**, *31*, 513.

[18] P. Howard, J. Tunkel, *Identification of CFC and HCFC substitutes for blowing polyurethane foam insulation products*. Washington, DC, **1995**.

[19] Y. Ohara, K. Tanaka, T. Hayashi, H. Tomita, S. Motani, *BCSJ* **2004**, *77*, 599.

[20] P. Ashford, M. W. Q. Guzma, *J. Cell. Plast.* **2004**, *40*, 255.

[21] J. Grünewald, P. Parlevliet, V. Altstädt, *J. Thermoplast. Compos. Mater.* **2017**, *30*, 437.

[22] C. B. Park, L. K. Cheung, *Polym. Eng. Sci.* **1997**, *37*, 1.

[23] G. J. Nam, J. H. Yoo, J. W. Lee, *J. Appl. Polym. Sci.* **2005**, *96*, 1793.

[24] H. E. Naguib, C. B. Park, U. Panzer, N. Reichelt, *Polym. Eng. Sci.* **2002**, *42*, 1481.

[25] G. Petrone, V. D'Alessandro, F. Franco, B. Mace, S. de Rosa, *Compos. Struct.* **2014**, *113*, 362.

[26] B. Jeong, M. Xanthos, Y. Seo, *J. Cell. Plast.* **2006**, *42*, 165.

[27] S.-T. Lee, M. Xanthos, S. K. Dey, *Foam Extrusion*, CRC Press, Boca Raton **2014**, p. 506.

[28] M. Xanthos, Q. Zhang, S. K. Dey, Y. Li, U. Yilmazer, M. O'Shea, *J. Cell. Plast.* **1998**, *34*, 498.

[29] J. Reignier, R. Gendron, M. F. Champagne, *J. Cell. Plast.* **2007**, *43*, 459.

[30] E. Di Maio, G. Mensitieri, S. Iannace, L. Nicolais, W. Li, R. W. Flumerfelt, *Polym. Eng. Sci.* **2005**, *45*, 432.

[31] P. Li, X. Zhu, M. Kong, Y. Lv, Y. Huang, Q. Yang, G. Li, *Int. J. Biol. Macromol.* **2021**, *183*, 222.

[32] X. Chen, J. Li, A. Pizzi, E. Fredon, C. Gerardin, X. Zhou, G. Du, *Ind. Crops Prod.* **2021**, *168*, 113607.

[33] X. Ye, A. J. Capezza, V. Gowda, R. T. Olsson, C. Lendel, M. S. Hedenqvist, *Adv. Sustainable Syst.* **2021**, *5*, 2100063.

[34] M. Nofar, C. B. Park, *Polylactide Foams: Fundamentals, Manufacturing, and Applications*, William Andrew, Norwich **2017**.

[35] P. T. Anastas, J. B. Zimmerman, *Environ. Sci. Technol.* **2003**, *37*, 94A.

[36] M. S. M. Alger, *Polymer Science Dictionary*, Chapman & Hall, London **1997**.

[37] O. Olabisi, K. Adewale, *Handbook of Thermoplastics*, CRC Press, Boca Raton **2016**.

[38] G. Bornmann, A. Loeser, *Arch. Toxikol.* **1968**, *23*, 240.

[39] I. Weidlich, in *Rohrleitungen 1* (Eds: H.-B. Horlacher, U. Helbig), Springer Berlin Heidelberg, Berlin, Heidelberg **2016**, p. 475.

[40] CEN. EN 253:2020–03, District heating pipes—bonded single pipe systems for directly buried hot water networks—factory made pipe assembly of steel service pipe, polyurethane thermal insulation and a casing of polyethylene; Beuth Verlag GmbH: Berlin.

[41] CEN. District heating pipes–pre-insulated flexible pipe systems–part 2: Bonded plastic service pipes—requirements and test methods: Brussels, Belgium: **2010**.

[42] E. Di Maio, E. Kiran, *J. Supercrit. Fluids* **2018**, *134*, 157.

[43] S. Doroudiani, C. B. Park, M. T. Kortschot, *Polym. Eng. Sci.* **1996**, *36*, 2645.

[44] L. Doyle, I. Weidlich, Recyclable insulating foams for high temperature applications. In Proc. of The First Int. Conf. on "Green" Polymer Materials **2020**; MDPI: Basel, Switzerland, May 2020–11/25/2020, p 7200.

[45] H. E. Naguib, C. B. Park, N. Reichelt, *J. Appl. Polym. Sci.* **2004**, *91*, 2661.

[46] M. Xanthos, S. K. Dey, Q. Zhang, J. Quintans, *J. Cell. Plast.* **2000**, *36*, 102.

[47] A. R. Berens, G. S. Huvard, in *Supercritical Fluid Science and Technology*, Vol. 406 (Eds: K. P. Johnston, J. M. L. Penninger), American Chemical Society, Washington, DC **1989**, p. 207.

[48] G. Natta, P. Corradini, I. W. Bassi, *Nuovo Cimento* **1960**, *15*, 52.

[49] A. T. Jones, *J. Polym. Sci. B Polym. Lett.* **1963**, *1*, 455.

[50] J. Boor, J. C. Mitchell, *J. Polym. Sci. A Gen. Pap.* **1963**, *1*, 59.

[51] C. Hadinata, D. Boos, C. Gabriel, E. Wassner, M. Rüllmann, N. Kao, M. Laun, *J. Rheol.* **2007**, *51*, 195.

[52] J. Crank, G. S. Park Eds., *Diffusion in Polymers*, Academic Press, London **1981**.

[53] J. Schindelin, I. Arganda-Carreras, E. Frise, V. Kaynig, M. Longair, T. Pietzsch, S. Preibisch, C. Rueden, S. Saalfeld, B. Schmid, J.-Y. Tinevez, D. J. White, V. Hartenstein, K. Eliceiri, P. Tomancak, A. Cardona, *Nat. Methods* **2012**, *9*, 676.

[54] H. Liu, X. Wang, W. Liu, B. Liu, H. Zhou, W. Wang, *Cell. Polym.* **2014**, *33*, 189.

[55] S. Takahashi, J. C. Hassler, E. Kiran, *J. Supercrit. Fluids* **2012**, *72*, 278.
[56] M. T. Ngo, J. S. Dickmann, J. C. Hassler, E. Kiran, *J. Supercrit. Fluids* **2016**, *109*, 1.
[57] W. Kaewmesri, P. C. Lee, C. B. Park, J. Pumchusak, *J. Cell. Plast.* **2006**, *42*, 405.
[58] E. Laguna-Gutierrez, J. Escudero, V. Kumar, M. A. Rodriguez-Perez, *J. Cell. Plast.* **2018**, *54*, 257.
[59] L. M. Matuana, O. Faruk, C. A. Diaz, *Bioresour. Technol.* **2009**, *100*, 5947.
[60] S.-T. Lee, B. P. Chul, *Foam Extrusion*, Taylor & Francis Inc, Bosa Roca **2014**.
[61] E. Kiran, *J. Supercrit. Fluids* **2010**, *54*, 296.
[62] L. A. Utracki, Z. Bakerdjian, M. R. Kamal, *J. Appl. Polym. Sci.* **1975**, *19*, 481.
[63] H. Münstedt, *Int. Polym. Process.* **2018**, *33*, 594.
[64] M. Xanthos, V. Tan, A. Ponnusamy, *Polym. Eng. Sci.* **1997**, *37*, 1102.
[65] P. Gong, S. Zhai, R. Lee, C. Zhao, P. Buahom, G. Li, C. B. Park, *Ind. Eng. Chem. Res.* **2018**, *57*, 5464.
[66] J. G. Burt, *J. Cell. Plast.* **1978**, *14*, 341.
[67] Z.-M. Xu, X.-L. Jiang, T. Liu, G.-H. Hu, L. Zhao, Z.-N. Zhu, W.-K. Yuan, *J. Supercrit. Fluids* **2007**, *41*, 299.
[68] P. Spitael, C. W. Macosko, *Polym. Eng. Sci.* **2004**, *44*, 2090.
[69] M. Antunes, J. I. Velasco, V. Realinho, E. Solórzano, *Polym. Eng. Sci.* **2009**, *49*, 2400.
[70] J. Zhao, Q. Zhao, C. Wang, B. Guo, C. B. Park, G. Wang, *Mater. Des.* **2017**, *131*, 1.
[71] C. P. Parky, G. A. Garcia, *J. Cell. Plast.* **2002**, *38*, 219.
[72] A. Farthi, *Mechanical Properties of Strand PET Foams at Different Length Scales*, Universität Bayreuth, Bayreuth **2018**. https://epub.uni-bayreuth.de/4286/.
[73] L. Di Maio, I. Coccorullo, S. Montesano, L. Incarnato, *Macromol. Symp.* **2005**, *228*, 185.

How to cite this article: L. Doyle, *J. Appl. Polym. Sci.* **2022**, *139*(12), e51816. https://doi.org/10.1002/app.51816